ELSEVIER

Journal of Nuclear Materials 247 (1997) 309–314

journal of nuclear materials

Thermal analysis of pseudo-binary system: LiCl–KCl eutectic and lanthanide trichloride

Kinya Nakamura *, Masaki Kurata

Central Research Institute of Electric Power Industry (CRIEPI), 11-1, Iwado-kita 2-chome, Komae-shi, Tokyo 201, Japan

Abstract

The phase diagrams of the pseudo-binary systems of LiCl–KCl eutectic and lanthanide trichloride ($LnCl_3$: Ln = La, Ce, Pr, Nd, Sm, and Gd) were determined for compositions less than 25 mol% $LnCl_3$ by means of thermal analysis, visual observation, electromotive force measurement and powder X-ray diffraction. The existence of K_2LnCl_5 compounds was confirmed in all the systems, but K_3LnCl_6 was observed only in the systems containing Sm and Gd. In the region up to 17 mol% $LnCl_3$, the eutectic temperature and composition were observed to be close to those of the LiCl–KCl eutectic system (625 ± 1 K, LiCl–41 at.% KCl). For compositions greater than 17 mol% $LnCl_3$, on the other hand, the eutectic points were 701 ± 1, 691 ± 1, 681 ± 1, 656 ± 1, 635 ± 1 and 649 ± 1 K for La, Ce, Pr, Nd, Sm, and Gd, respectively. The liquidus surface of the LiCl–KCl–$LaCl_3$ system was also determined at compositions up to 40 mol% $LnCl_3$.

1. Introduction

A pyrometallurgical process has been developed for partitioning transuranium elements (TRUs) contained in high-level radioactive liquid waste (HLLW), which is generated in the reprocessing of LWR spent fuels [1–3]. Since the pyrometallurgical process, electrorefining and/or reductive extraction, is carried out in a molten salt system where the solvent is LiCl–KCl eutectic salt [4], knowledge of the phase diagrams of molten salt is very important for the process design. The phase diagram concerning lanthanide trichloride, $LnCl_3$, is particularly important, because of the larger amount contained in HLLW as compared with TRUs and because of its chemical similarity to TRUs.

Bergmann et al. [5] reported the phase diagrams of the KCl–$LnCl_3$ binary system for Ln = La–Lu and K_2LnCl_5, K_3LnCl_6, and other compounds were formed at temperatures over 573 K. On the other hand, Seifert et al. [6–10] and Thiel and Seifert [11] pointed out that K_2LnCl_5 (Ln = La, Ce, Pr, Nd, Sm, and Gd), $K_3La_5Cl_{18}$ and KGd_2Cl_7 were stable from room temperature to their decomposition temperatures, but that the other compounds, such as K_3LnCl_6, existed only at higher temperatures.

The phase diagrams of the LiCl–$LnCl_3$ (Ln = La, Pr, Nd, and Sm) system have been reported in the literature [12–17] and only $LiSm_2Cl_7$ is considered a compound. The phase diagrams of the ternary systems have had few reports except for the LiCl–KCl–$NdCl_3$ system [15].

For a better understanding of the mixed salt system, we studied the phase diagrams of the LiCl–KCl eutectic and $LnCl_3$ pseudo-binary system in the region up to 25 mol% $LnCl_3$ by thermal analysis, visual observation, electromotive force (EMF) measurement and powder X-ray diffraction (XRD).

2. Experimental

The anhydrous salt reagents, such as $LnCl_3$ (Ln = La, Ce, Pr, Nd, Sm, and Gd), LiCl, KCl, and LiCl–KCl eutectic, were purchased from APL Engineered Materials. Their purities were 99.99%, except for $SmCl_3$ (99.95%).

The thermal analysis was performed with a differential scanning calorimeter installed in a globe box filled with a high purity argon atmosphere (< 0.5 ppm O_2 and < 0.1

* Corresponding author. Tel: +81-33 480 2111; fax: +81-33 480 2493; e-mail: kinya@criepi.denken.or.jp.

0022-3115/97/$17.00
PII S0022-3115(97)00099-8

ppm H_2O). The temperature calibration was accomplished by measuring the melting point of high purity metals, such as Sn, Pb, Zn, and Al (> 99.99%).

A fixed amount of the LiCl–KCl eutectic and $LnCl_3$ salt reagents were weighed in a high purity alumina cup and heated until melted for mixing. The salt was quickly cooled to room temperature and was used for thermal analysis. The heating rate was 1 K/min and an empty alumina cup was used as a reference. The compositions of the sample were determined by ICP-AES and atomic absorption spectroscopy after the thermal analysis.

The liquidus temperature of the salt samples was visually measured by heating them in a transparent furnace. Details of the apparatus have been described elsewhere [18]. The salt samples, sealed in quartz tubes, were melted for mixing and then quickly cooled to room temperature. They were heated at 5 K increments and kept for several hours for equilibrium. We verified complete melting of the samples with microscopic examinations.

The chemical form of the salt samples at room temperature was determined from powder XRD analysis. The primary phase, the first crystalline phase to appear from the liquid state on cooling, was determined from EMF measurement in an electrochemical cell; La|$LaCl_3$, LiCl–KCl||AgCl, LiCl–KCl|Ag. The details have been given elsewhere [19].

3. Results and discussion

3.1. Pseudo-binary system: LiCl–KCl eutectic and $LaCl_3$

Representative thermograms for the sample containing LiCl–KCl eutectic and $LaCl_3$ obtained on heating are shown in Fig. 1. Three types of endothermic peaks are observed in each thermogram. Since the onset temperature of the first peak, designated 'A' in Fig. 1, hardly changed with an increase in the $LaCl_3$ concentration, we assigned the onset temperature to the eutectic points. Those are 625 ± 1 and 701 ± 1 K for compositions less than and greater than 17 mol% $LaCl_3$, respectively. The difference in the eutectic points corresponds to the difference in components concerning these eutectic reactions. The invariant temperatures reveal the freedom, $f = 0$ in the reaction.

The second peak, designated 'B', gradually separated from the baseline with an increase in temperature and after peaking quickly approached the baseline. The baseline is a thermogram when the difference in the temperature between the sample and reference equals zero. The third peak, designated 'C', also exhibited a gradual change. Therefore, peaks 'B' and 'C' can be attributed to the phase transitions accompanying the decrease in the number of the phase, revealing $f = 1$. We have determined that the peak temperature of the second and third peaks is the transition temperature.

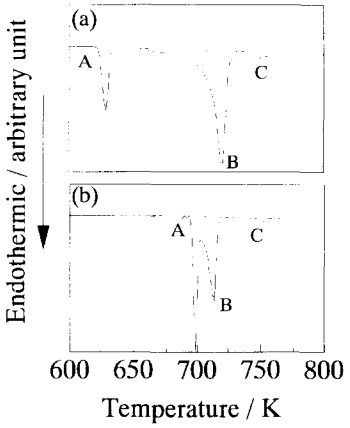

Fig. 1. Thermogram of the pseudo-binary system: LiCl–KCl eutectic and $LaCl_3$. (a) 13.2 mol% $LaCl_3$ and (b) 20.4 mol% $LaCl_3$. The dashed lines (---) indicate the baseline of thermal analysis.

Fig. 2 illustrates the results of the thermal analysis and the visual observations of the samples consisting of LiCl–KCl eutectic and $LaCl_3$. The liquidus temperature shows a maximum at 17 mol% $LaCl_3$. The values obtained from the visual observations are in good agreement with those of the thermal analysis with the exception of the region around 17 mol% $LaCl_3$, where the differences are as large as 15 K. These differences might be due to a slower melting rate of the salt sample than the heating rate of 1 K/min used in the thermal analysis.

We investigated the chemical form of the primary phase by EMF measurement. The relationship of the La potential in the molten salt to temperature is shown in Fig. 3. The EMF values decrease linearly with decreasing temperature. Inflection points are observed at 699 ± 3 and 712 ± 3 K for 4.4 and 7.4 mol% $LaCl_3$, respectively. These are reasonably consistent with the liquidus temperatures obtained by thermal analysis, which are designated 'a' and 'b' in Fig. 3. Below the inflection points, the derived potentials are lower than the extrapolated values from high temperature, shown by dashed lines. Since the decrease in potential at each temperature corresponds to a decrease in La concentration, La rich compounds are considered to be precipitated below the liquidus temperatures.

According to powder XRD patterns, LiCl, K_2LaCl_5, and KCl were detected in the region up to 17 mol% $LaCl_3$. This revealed that the eutectic reaction originated from these compounds. However, LiCl and K_2LaCl_5 only were detected in the region above 17 mol% $LaCl_3$.

The value 17 mol% $LaCl_3$ in the pseudo-binary system geometrically corresponds to the intersection of two straight lines on the composition triangle of a ternary LiCl–KCl–$LaCl_3$ system, one connects LiCl and K_2LaCl_5 and the other connects the LiCl–KCl eutectic and $LaCl_3$. Hence, the composition at 17 mol% $LaCl_3$ in the pseudo-binary

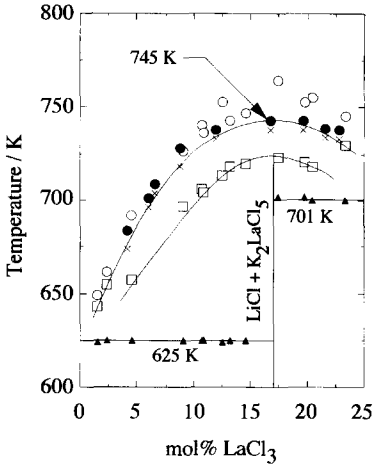

Fig. 2. Partial phase diagram of pseudo-binary system: LiCl–KCl eutectic and $LaCl_3$. The symbols ▲, □ and ○ indicate three types of transitions determined by thermal analysis and the symbols ● and × indicate liquid and two-phase regions determined by visual observations, respectively.

system is considered to be a mixture of LiCl and K_2LaCl_5 because a binary LiCl–K_2LaCl_5 system is considered to be a eutectic system.

Consequently, the phase transitions designated 'A', 'B' and 'C' in Fig. 1 in the region below 17 mol% $LaCl_3$ are identified by the following reactions:

A: $K_2LaCl_5 + LiCl + KCl \rightarrow K_2LaCl_5 + LiCl + L$,

B: $K_2LaCl_5 + LiCl + L \rightarrow K_2LaCl_5 + L$,

C: $K_2LaCl_5 + L \rightarrow L$,

where L represents the liquid phase.

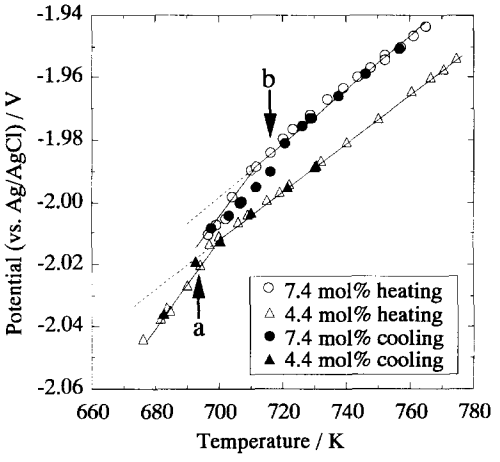

Fig. 3. Temperature dependency of La potential against Ag/AgCl reference electrode. The symbols designated 'a' and 'b' indicate the liquidus temperatures of the 4.4 and 7.4 mol% $LaCl_3$ samples, respectively. These values were obtained by thermal analysis.

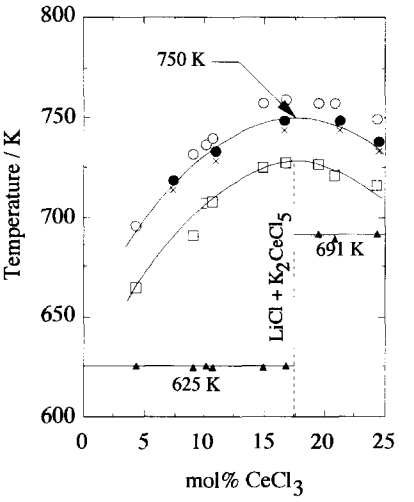

Fig. 4. Partial phase diagram of pseudo-binary system: LiCl–KCl eutectic and $CeCl_3$. See Fig. 2 caption for symbols.

3.2. Pseudo-binary system: LiCl–KCl eutectic and $LnCl_3$ (Ln = Ce, Pr, Nd, Sm, and Gd)

Figs. 4–6 illustrate partial phase diagrams of the pseudo-binary systems of Ce, Pr, and Nd, respectively, obtained in the same manner as the La system. As observed in the La system, K_2LnCl_5 was formed in the region up to 17 mol% $LnCl_3$. For compositions greater than 17 mol% $LnCl_3$, however, slightly different eutectic points, 701 ± 1, 691 + 1, 681 ± 1, and 656 ± 1 K for La, Ce, Pr, and Nd, respectively, were observed.

The phase diagrams of LiCl–KCl eutectic and $SmCl_3$ and LiCl–KCl eutectic and $GdCl_3$ pseudo-binary systems are shown in Figs. 7 and 8, respectively. The change of the

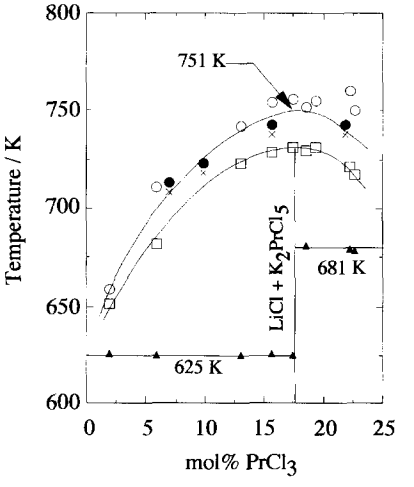

Fig. 5. Partial phase diagram of pseudo-binary system: LiCl–KCl eutectic and $PrCl_3$. See Fig. 2 caption for symbols.

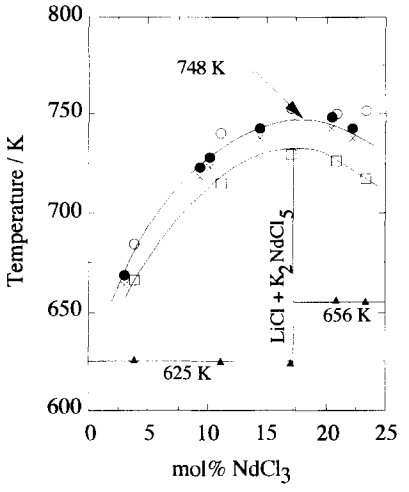

Fig. 6. Partial phase diagram of pseudo-binary system: LiCl–KCl eutectic and $NdCl_3$. See Fig. 2 caption for symbols.

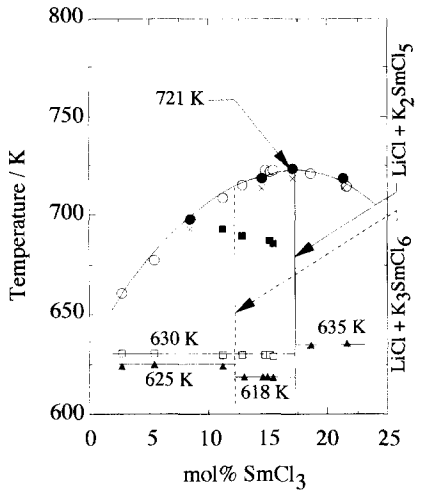

Fig. 7. Partial phase diagram of pseudo-binary system: LiCl–KCl eutectic and $SmCl_3$. See Fig. 2 caption for symbols.

eutectic point is observed around 12 mol% $LnCl_3$ in both systems. This suggests the presence of K_3LnCl_6 type of compounds, because the point in the pseudo-binary system geometrically corresponds to the intersection of two straight lines on the composition triangle of a ternary LiCl–KCl–$LnCl_3$ system: one connects LiCl and K_3LnCl_6 and the other connects the LiCl–KCl eutectic and $LnCl_3$. For the Gd system, moreover, the existence of K_3GdCl_6 is supported by the derived phase diagram showing the maximum liquidus temperature at 12 mol% $GdCl_3$. According to Seifert [10] and Theil and Seifert [11], the formation temperatures of K_3SmCl_6 and K_3GdCl_6 are 611 and 548 K, respectively, which are much lower than the liquidus temperatures shown in Figs. 7 and 8.

The solubilities of $LnCl_3$ in LiCl–KCl eutectic are determined from the phase diagrams. They are about 3 mol% $LnCl_3$ at 673 K except for Sm and it is about 4 mol% $SmCl_3$. At 723 K, they are about 9 mol% for La, Ce, Pr, and Nd and are above 25 mol% for Sm and Gd.

3.3. The ternary LiCl–KCl–$LaCl_3$ and LiCl–KCl–$NdCl_3$ systems

The liquidus surface in the ternary LiCl–KCl–$LaCl_3$ system in the region below 40 mol% $LaCl_3$ is shown in Fig. 9. The liquidus surface is composed of four primary crystallization areas for the LiCl, KCl, K_2LaCl_5, and $LaCl_3$ phases. It exhibits three invariant equilibrium reactions related to E_1^{La}, E_2^{La}, and P_1^{La}, respectively, in Fig. 9:

$$E_1^{La}: L \leftrightarrows LiCl + KCl + K_2LaCl_5,$$

$$E_2^{La}: L \leftrightarrows LiCl + K_2LaCl_5 + K_3La_5Cl_{18},$$

$$P_1^{La}: L + LaCl_3 \leftrightarrows LiCl + K_3La_5Cl_{18}.$$

The symbols of E and P represent a eutectic and a peritectic reaction, respectively. The point of E_1^{La} (625 ± 1 K) is located in the periphery of the eutectic composition of the LiCl–KCl system. Judging from the results of the EMF measurement, the composition of E_2^{La} (701 ± 1 K) is located in the region rich in LiCl.

The liquidus surface in the ternary LiCl–KCl–$NdCl_3$ system reported by Zhang et al. [15] is shown in Fig. 10. Our results are in good agreement with those of Zhang et al. except at the eutectic points.

The liquidus surface of the LiCl–KCl–$CeCl_3$ and LiCl–KCl–$PrCl_3$ systems would be similar to that of the LiCl–KCl–$NdCl_3$ system because of the similarity of the

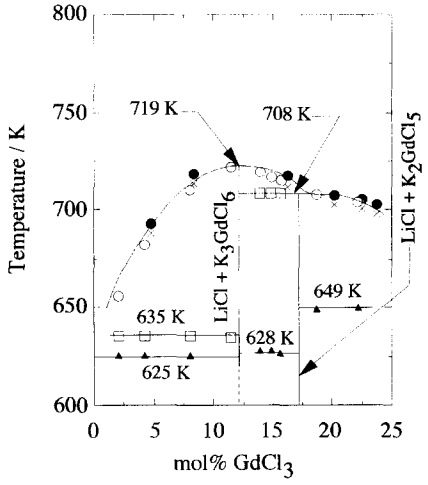

Fig. 8. Partial phase diagram of pseudo-binary system: LiCl–KCl eutectic and $GdCl_3$. See Fig. 2 caption for symbols.

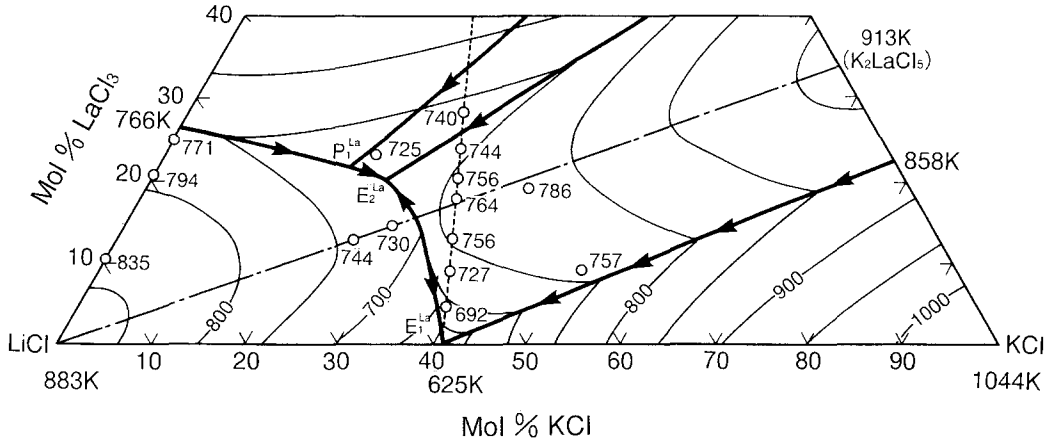

Fig. 9. Partial phase diagram of the ternary LiCl–KCl–$LaCl_3$ system. Open circles are liquidus temperatures obtained by thermal analysis. The symbols designated as E_i^{La} and P_i^{La} are eutectic and peritectic compositions, respectively.

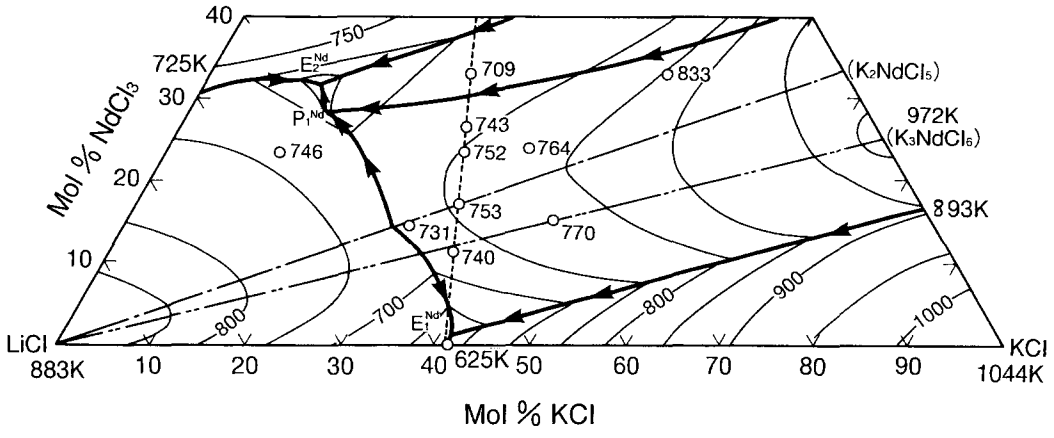

Fig. 10. Partial phase diagram of the ternary LiCl–KCl–$NdCl_3$ system reported by Zhang et al. [15] (with permission). Open circles are liquidus temperatures obtained by thermal analysis. The symbols designated as E_i^{Nd} and P_i^{Nd} are the eutectic compositions in the ternary system.

derived pseudo-binary phase diagrams, as shown in Figs. 4–6 and because of the similarity of the KCl–$LnCl_3$ binary systems [6–11].

4. Conclusions

The phase diagrams of the pseudo-binary systems, LiCl–KCl eutectic and $LnCl_3$ (Ln = La, Ce, Pr, Nd, Sm, and Gd), in the region below 25 mol% $LnCl_3$ were determined by four analytical methods, thermal analysis, visual observation, EMF measurement, and powder XRD. The following conclusions can be drawn.

(1) The K_2LnCl_5 was found in all systems and the compound K_3SmCl_6 and K_3GdCl_6 were considered to exist in the Sm and Gd systems, respectively.

(2) The eutectic points of the La, Ce, Pr, and Nd systems were all 625 ± 1 K in the region up to 17 mol% $LnCl_3$ and 701 ± 1, 691 ± 1, 681 ± 1, and 656 ± 1 K, respectively, in the region above 17 mol% $LnCl_3$. The eutectic points of the Sm and Gd systems were 625 ± 1 K in the region up to 12 mol% $LnCl_3$ for both systems, 618 ± 1 and 628 ± 1 K in the range between 12 and 17 mol% $LnCl_3$, and 635 ± 1 and 649 ± 1 K in the region above 17 mol% $LnCl_3$, respectively.

(3) Three transition peaks for the LiCl–KCl eutectic and $LaCl_3$ system were identified up to 17 mol% $LaCl_3$.

The liquidus surface in the ternary LiCl–KCl–$LaCl_3$ system in the region below 40 mol% $LaCl_3$ was determined and that of the LiCl–KCl–$NdCl_3$ system was compared with one previously reported.

Acknowledgements

The authors are greatly indebted to Associate Professor Dr Y. Sato of the Department of Metallurgy of Tohoku

University for his worthy suggestions. They are also thankful to Dr K. Kobayashi of Sumitomo Metal Mining Co. and our colleagues in CRIEPI for many fruitful discussions.

References

[1] T. Inoue, M. Sakata, H. Miyashiro, A. Sasahara, T. Matsumura, Nucl. Technol. 93 (1991) 206.
[2] T. Inoue, M. Sakata, M. Kurata, Y. Sakamura, T. Hijikata, K. Kinoshita, IAEA-TECDOC-783, 1995, p. 137.
[3] M. Kurata, Y. Sakamura, K. Kinoshita, T. Higashi, Proc. Int. Conf. on Evaluation of Emerging Nuclear Fuel Cycle Systems, Vol. 1, Versailles, France, Sept. 11–14, 1995, pp. 1067–1071.
[4] Y. Sakamura, T. Inoue, T.S. Storvick, L.F. Grantham, Proc. Int. Conf. on Evaluation of Emerging Nuclear Fuel Cycle Systems, Vol. 2, Versailles, France, Sept. 11–14, 1995, pp. 1185–1192.
[5] H. Bergmann, U. Vetter, E. Best, Gmelin Handbuch der Anorganischen Chemie, Vol. 39 (Springer, Berlin, 1977) (in German).
[6] H.J. Seifert, H. Fink, G. Thiel, J. Less Common Met. 110 (1985) 139.
[7] H.J. Seifert, J. Sandrock, G. Thiel, J. Therm. Anal. 31 (1986) 1309.
[8] H.J. Seifert, J. Sandrock, J. Uebach, Z. Anorg. Allg. Chem. 555 (1987) 143, in German.
[9] H.J. Seifert, H. Fink, J. Uebach, J. Therm. Anal. 33 (1988) 625.
[10] H.J. Seifert, J. Sandrock, G. Thiel, Z. Anorg. Allg. Chem. 598&599 (1991) 307, in German.
[11] G. Thiel, H.J. Seifert, Thermochim. Acta 133 (1988) 275.
[12] C.-G. Zheng, Y.-P. Chen, L.-P. Zhang, Chin. Sci. Bull. 39 (6) (1994) 480.
[13] Z. Qiao, M. Wang, S. Duan, C. Zheng, Acta Metall. Sin. 25 (4) (1989) 234, in Chinese.
[14] Y.-F. Zhang, C.-G. Zheng, Y.-P. Ye, Acta Chim. Sin. 47 (1) (1989) 14, in Chinese.
[15] Y.-F. Zhang, C.-G. Zheng, Y.-P. Ye, Acta Metall. Sin. 24 (4) (1988) 243, in Chinese.
[16] C.-G. Zheng, J. Jin, Y.-P. Ye, Acta Chim. Sin. 47 (7) (1989) 678, in Chinese.
[17] Y.-F. Zhang, B. Meng, Acta Chim. Sin. 49 (9) (1991) 839, in Chinese.
[18] Y. Sato, T. Eshima, J. Japan Inst. Metals 42 (9) (1978) 905, in Japanese.
[19] Y. Sakamura, H. Miyashiro, S. Matsumoto, CRIEPI report T91003, 1991 (in Japanese).